



## Magnetic topology and current channels in plasmas with toroidal current density inversions

D. Ciro and I. L. Caldas

Citation: [Physics of Plasmas \(1994-present\)](#) **20**, 102512 (2013); doi: 10.1063/1.4825241

View online: <http://dx.doi.org/10.1063/1.4825241>

View Table of Contents: <http://scitation.aip.org/content/aip/journal/pop/20/10?ver=pdfcov>

Published by the [AIP Publishing](#)

---



## Re-register for Table of Content Alerts

Create a profile.



Sign up today!



# Magnetic topology and current channels in plasmas with toroidal current density inversions

D. Ciro<sup>a)</sup> and I. L. Caldas

*Departamento de Física Aplicada, Universidade de São Paulo, 05508-090 São Paulo, Brazil*

(Received 9 August 2013; accepted 2 October 2013; published online 16 October 2013)

The equilibrium magnetic field inside axisymmetric plasmas with inversions on the toroidal current density is considered. Previous works have shown that internal regions with negative current density lead to non-nested magnetic surfaces inside the plasma. Following these results, we derive a general expression relating the positive and negative currents inside the non-nested surfaces. This is done in terms of an anisotropy parameter that is model-independent and is based in very general properties of the magnetic field. We demonstrate that the positive currents in axisymmetric islands screen the negative one in the plasma center by reaching about twice its magnitude. Further, we illustrate these results by developing a family of analytical local solutions for the poloidal magnetic field in a region of interest that contains the inverted current. These local solutions exhibit non-nested magnetic surfaces with a combined current of at least twice the magnitude of the negative one, as prescribed from the topological arguments, and allow to study topological transitions driven by geometrical changes in the current profile. To conclude, we discuss the signatures of internal current density inversions in a confinement device and show that magnetic pitch measurements may be inappropriate to differentiate current reversals and small current holes in plasmas. © 2013 AIP Publishing LLC. [<http://dx.doi.org/10.1063/1.4825241>]

## I. INTRODUCTION

In tokamak devices, the toroidal magnetic field confine the orbits of the charged particles inside a chamber. A toroidal current induced within the plasma produces the poloidal magnetic field that prevent particle drift losses. Additional heating coming from non-inductive drive mechanisms help to sustain the plasma current for longer pulses with small or negative inductive drive and during slow transitions from positive to negative plasma current.<sup>1</sup> These configurations are relevant to the improvement of the confinement times and the search for steady-state operation regimes. A relevant question arising from this situations is that of the structure of the magnetic field when the toroidal current density becomes negative in some region inside the plasma. In the last decade, the achievement of quasi-steady-state alternating current scenarios,<sup>2</sup> the observation of internal vanishing current densities<sup>3</sup> and stiff current density holes (finite regions with near zero current density at the plasma center),<sup>4</sup> have attracted attention to the problem of current reversal equilibrium configurations (CRECs).

From different numerical and analytical approaches,<sup>5–8</sup> it has been observed that internal current density reversals lead to an equilibrium magnetic field consisting of axisymmetric magnetic islands around a central nested structure with a principal magnetic axis. However, the understanding of the magnetic islands number and sizes is usually restricted to the particular model employed to describe the equilibrium. In this direction, a more generic topological treatment independent of particular hydromagnetic models is desirable. To achieve this, we split the magnetic topology into current

channels through the magnetic separatrix and study the relation between the currents in these channels. Such treatment is independent of the magnetic topology and leads to very general statements about the current distribution inside the system.

In this work, we demonstrate that, in general, the total current inside the islands have about twice the magnitude of the negative current in the center. This result is obtained by the introduction of an anisotropy parameter that is related to the geometric properties of the magnetic islands. Further, we illustrate such relation by developing a local description of the magnetic field with two geometric parameters. The solution to the equilibrium problem is obtained without specifying further plasma profiles or arbitrary functions and is valid in a region of interest where the toroidal current density is both positive and negative. The obtained configurations not only agree with several published topologies<sup>5–8</sup> but also allow to identify transitions between different magnetic configurations by changes in the anisotropy. We also show that the characteristic flattening on the magnetic pitch measurements usually interpreted as a current hole may be also produced by a small current density reversal, indicating that additional diagnostics other than Motional Stark Effect (MSE) may be required to distinguish between current holes and reversed currents.

## II. EQUILIBRIUM FIELD TOPOLOGY

### A. Non-nested magnetic surfaces

Let us start by writing the magnetic field for any axisymmetric system in the form

$$\mathbf{B} = \nabla\psi \times \nabla\phi + F\nabla\phi, \quad (1)$$

<sup>a)</sup>Electronic mail: davidcirotaborda@usp.br.

where  $\psi(R, z) = RA_\phi(R, z)$  and  $F(R, z) = RB_\phi(R, z)$  are proportional to the poloidal magnetic flux and poloidal current, respectively.  $B_\phi(R, z)$  and  $A_\phi(R, z)$  are the toroidal components of the magnetic field and vector potential and  $(R, \phi, z)$  are the usual cylindrical coordinates. The term  $\nabla\psi \times \nabla\phi$  corresponds to the poloidal component of the magnetic field  $\mathbf{B}_p$ , that rests in any plane  $\phi = \text{const}$ . From,  $\mathbf{B} \cdot \nabla\psi = 0$ , it is clear that the magnetic field lines are attached to the level sets of  $\psi(R, z)$ , the so called *magnetic surfaces*. In usual tokamak configurations, these surfaces form a single family of nested tori inside the plasma.

The total current flowing inside a torus labeled by  $\psi$  is obtained from the Ampère's law and Eq. (1) as

$$\mu_0 I_r(\psi) = \oint_{\Gamma_\psi} \mathbf{B} \cdot d\mathbf{l} = \pm \oint_{\Gamma_\psi} |\nabla\psi| \frac{dl}{R}, \quad (2)$$

where  $dl$  follows clockwise the *magnetic circuit*  $\Gamma_\psi$ , defined as the intersection of the torus  $\psi$  with any azimuthal plane  $\phi = \text{const}$ . The current is negative when  $\nabla\psi$  is inwards and positive otherwise (Fig. 1).

The possibility of both positive and negative current densities in a single equilibrium configuration suggests the existence of some torus  $\psi_0$  containing a net vanishing current, however, the rightmost integrand in Eq. (2) is positive definite, requiring  $|\nabla\psi| = 0$  in every point of the torus  $\psi_0$ . Such degeneracy<sup>9</sup> is possible for one-dimensional problems, but leads to structural instability in two-dimensions,<sup>7</sup> i.e., any variation in the poloidal field will destroy the topology of the torus  $\psi_0$ . This indicates that the usual nested topology is not compatible with current density reversals in two dimensions.

A more feasible configuration, i.e., structurally stable, requires that  $\nabla\psi(R, z)$  vanishes at several isolated points,  $n$  saddles and  $n + 1$  centers. Each saddle leads to a poloidal field inversion and introduces four branches where the condition  $\psi(R, z) = \psi_s$  is satisfied, with  $\psi_s$  the value of the poloidal flux on the saddle.

The magnetic topology depends on how the separatrix  $\Gamma_s = \Gamma_{\psi_s}$  connects two branches of the same hyperbolic point when followed smoothly. If  $\Gamma_s$  connects two

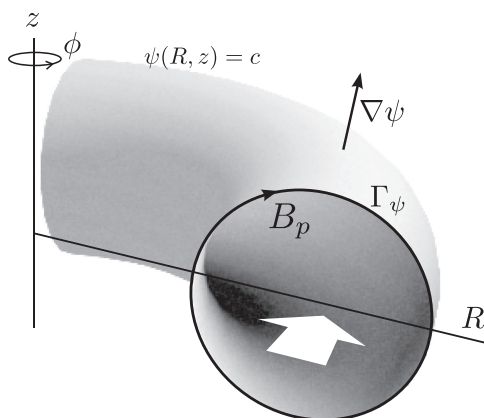


FIG. 1. Magnetic surface containing a net positive current. The poloidal field is clockwise as expected and encloses the internal current (white arrow).

non-opposite branches of any saddle the total number of saddles is odd (Fig. 2(a)). On the other hand, when  $\Gamma_s$  connects two opposite branches the number of saddles is even (Fig. 2(b)). The separatrix delimits several families of nested magnetic surfaces, each working as a *current channel* inside the plasma. These axisymmetric channels are also called *non-nested surfaces* in the literature. In Fig. 2, the poloidal field direction reveals the sign of the toroidal current inside the channels of different configurations with current density reversals.

The central channel contains a negative current, therefore, it encloses mostly a region with negative current density. The opposite happen for the remaining channels with positive current. As the poloidal field never inverts in a regular magnetic surface, its line integral on a finite magnetic circuit will never vanish. From this, a circuit just enclosing all the channels contains a finite positive current, meaning that the total current in the positive channels must exceed the current of the negative one. In the following, we make this more precise.

### B. Screening of the negative current

Each positive channel is bounded by the separatrix and two hyperbolic points and contains at least one elliptic point. We can always build a curve  $\gamma$  orthogonal to the magnetic field (Fig. 3(a)) that passes through all the hyperbolic and elliptic points that define the positive current channels (Fig. 3(b)).

The non-magnetic circuit  $\gamma$  splits in two every positive channel and satisfies  $\mathbf{B}_p \cdot d\mathbf{l} = 0$ . In other words  $\gamma$  encloses a vanishing current, since  $\oint_\gamma \mathbf{B}_p \cdot d\mathbf{l} = 0$ . Considering the separatrix  $\Gamma_s$  as composed of a pair of simple circuits  $\{\Gamma_1, \Gamma_2\}$  (Fig. 3(b)) it can be shown that

$$-\oint_{\Gamma_1} B_p dl = \sum_i I_1^i \equiv I_1, \quad \oint_{\Gamma_2} B_p dl = \sum_i I_2^i \equiv I_2, \quad (3)$$

with  $I_{1,2}^i$ , the current flowing through the area between  $\gamma$  and  $\Gamma_{1,2}$  in the  $i$ 'th positive channel (Fig. 3(a)). The  $i$ 'th positive current is  $I^i = I_1^i + I_2^i$  and the relative difference between its *half currents*,  $\eta_i = (I_2^i - I_1^i)/I^i$ , gives a measure of the anisotropy of the  $i$ 'th magnetic island. The total current inside all the positive channels is  $I_+ = I_1 + I_2$  and the current in the central channel is  $I_- = -I_1$ . Defining the mean anisotropy as  $\eta = \sum_i \eta_i I_i / \sum_i I_i$  and using the previous definitions we have

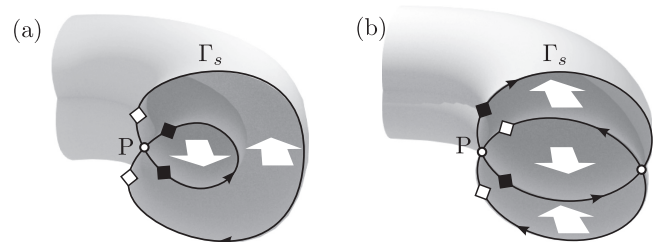


FIG. 2. Separatrix for odd (a) and even (b) systems of axisymmetric islands. Branches of the saddle P with corresponding diamonds are connected smoothly by the separatrix  $\Gamma_s$ . The direction of  $\mathbf{B}_p$  is indicated over the separatrix and the white arrows show the direction of the total current for each channel, the positive direction is entering the page.

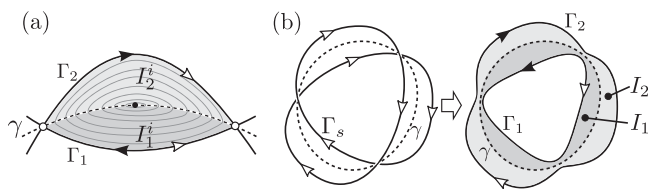


FIG. 3. (a) Splitting of the  $i$ 'th positive channel into its half-currents by the curve  $\gamma$ . (b) Decomposition of a separatrix into simple circuits and the regions for the currents in Eq. (3). Open arrows show the circuit orientation and simple ones the poloidal field direction.

$$I_+ = \frac{2}{1 - \eta} |I_-|. \tag{4}$$

For small anisotropies, we have  $I_+ \sim 2|I_-|$  and for regions with monotonic variation of the current density we expect  $0 \leq \eta_i < 1$ , leading to  $I_+ > 2|I_-|$ . This reveals that the current in the positive channels screen the negative current and the combined channels  $I_+ + I_-$  carry a net positive current larger than  $|I_-|$ .

### III. A FAMILY OF LOCAL SOLUTIONS

To study the size and number of magnetic islands in terms of the anisotropy, we need to put  $\eta$  in terms of other parameters of the equilibrium. For this, we develop a *local* solution that accounts for the non-nested topology while keeping a simplified physical picture of the equilibrium.

From Eq. (1) and  $\nabla \times \mathbf{B} = \mu_0 \mathbf{j}$ , it can be verified that

$$R \nabla \cdot (R^{-2} \nabla \psi) = -\mu_0 j_\phi. \tag{5}$$

Also, from the single-fluid MHD equilibrium<sup>10</sup> the force balance condition  $\nabla p = \mathbf{j} \times \mathbf{B}$ , leads to the relation

$$\mu_0 j_\phi = \mu_0 R p'(\psi) + R^{-1} F(\psi) F'(\psi), \tag{6}$$

where the prime denotes  $d/d\psi$ ,  $p(\psi)$  is the kinetic pressure and  $F(\psi)$  is defined after Eq. (1). Equations (5) and (6) give the well known Grad-Shafranov (G-S) equation.<sup>11,12</sup> To solve this nonlinear equation a self-consistent choice of the *surface functions*  $\{p(\psi), F(\psi)\}$  and boundary conditions is required. These definitions will characterize the equilibrium reached by the system.<sup>10</sup> In regular situations, the equilibrium is described by a unique family of magnetic surfaces, requiring a single choice of  $\{p(\psi), F(\psi)\}$  and a single boundary (the plasma edge). In the present work, we avoid that approach that may be unappropriated for the CRECs since they are composed of several magnetic families. However, at least formally, a single choice of the sources  $p(\psi)$  and  $F(\psi)$  may lead to current density inversions and multiple magnetic families.<sup>5,6</sup> In other approaches<sup>7,8</sup> the use of successive approximations with prescribed zero-order current density models and boundary conditions leads to the expected nonested topology.

Formally, a broad range of choices for the arbitrary functions  $p(\psi)$  and  $F(\psi)$  or zero-order profiles may lead to current reversals and non-nested configurations, but the underlying description of the equilibrium topology is not restricted to the particularly chosen model. In the present

work, we build a geometrical picture of the equilibrium by assuming directly the existence of a small negative minimum of the current density without setting the arbitrary functions. This will allow us to cover a wide range of situations without specifying the plasma state. With this approach, we also obtain a clear definition of the parameters that alter the topology of the magnetic field in the core of a current reversal plasma. It is important to mention that in the following calculations we do not solve the Grad-Shafranov equation (Eq. (5) subject to Eq. (6)), since it involves the specification of the hydromagnetic equilibrium through  $p(\psi)$  and  $F(\psi)$ . Instead, we solve Eq. (5) that correspond to the Ampère's law for an axisymmetric system.

In the following, we consider a hollow-current configuration possessing a very small negative current density in the core of the plasma. About the minimum at  $\mathbf{r}_0$  we can expand the current density as  $j_\phi(\mathbf{r}) \approx j_\phi(\mathbf{r}_0) + 1/2(\delta \mathbf{r} \cdot \nabla)_{\mathbf{r}_0}^2 j_\phi(\mathbf{r}) + O(\delta r^3)$ . For an up-down symmetric equilibrium, this can be casted like  $j_\phi = j_0 + \iota(r^2 - \kappa r^2 \cos^2 \theta) + O(r^3)$ , where  $(r, \theta)$  are local polar coordinates centered at  $\mathbf{r}_0 = (R_0, \phi, 0)$ . Here,  $j_0 = j(\mathbf{r}_0) < 0$ ,  $r = |\mathbf{r} - \mathbf{r}_0|$  and  $\theta$  is measured counterclockwise between  $e_R$  and  $\mathbf{r} - \mathbf{r}_0$ . The parameters  $\iota$  and  $\kappa$  are related to the curvature and ellipticity of  $j(r)$  about  $\mathbf{r}_0$ . In a first approximation, the poloidal field vanishes in a circle with radius  $a = \sqrt{-2j_0/\iota}$  enclosing a zero current and  $j_\phi$  vanishes at  $r = a/\sqrt{2}$ . As we are interested in the topology of the magnetic surfaces near a poloidal field reversal, we define a *region of interest* with radius  $a$ , centered at  $\mathbf{r}_0 = (R_0, \phi, 0)$  (Fig. 4).

Provided that  $a$  is small we can solve Eq. (5) by a *local* scheme analogous to the successive approximations method.<sup>10</sup> Nonetheless, in our case, the inverse aspect ratio  $\epsilon = a/R_0$ , is a reliably small parameter defined from the region of interest instead of the plasma radius  $a'$  (Fig. 4). Consequently, a fast convergence of the approximations is expected in the core of the plasma when the region of interest is not too large. In fact, if we are considering the possibility of a current inversion near a hollow configuration, the region of interest will be small and the following solutions apply.

Defining  $R = R_0 + ax$  and  $z = ay$  we can write Eq. (5) about the current minimum in dimensionless form

$$\left( \partial_x^2 + \partial_y^2 - \frac{\epsilon}{1 + \epsilon x} \partial_x \right) \psi = (1 + \epsilon x)(1 - 2r^2 + 2\kappa x^2), \tag{7}$$

with  $r$  measured in units of  $a$  and  $\psi$  in units of  $\mu_0 |j_0| a^2 R_0$ . The solutions of Eq. (7) will depend on the ellipticity  $\kappa$  and

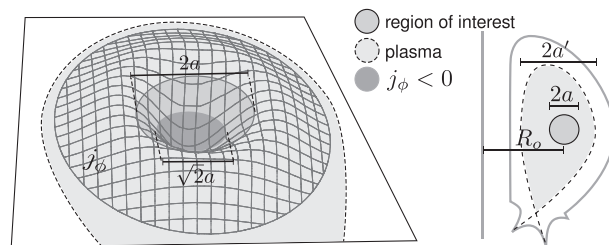


FIG. 4. Region of interest containing a negative current density.



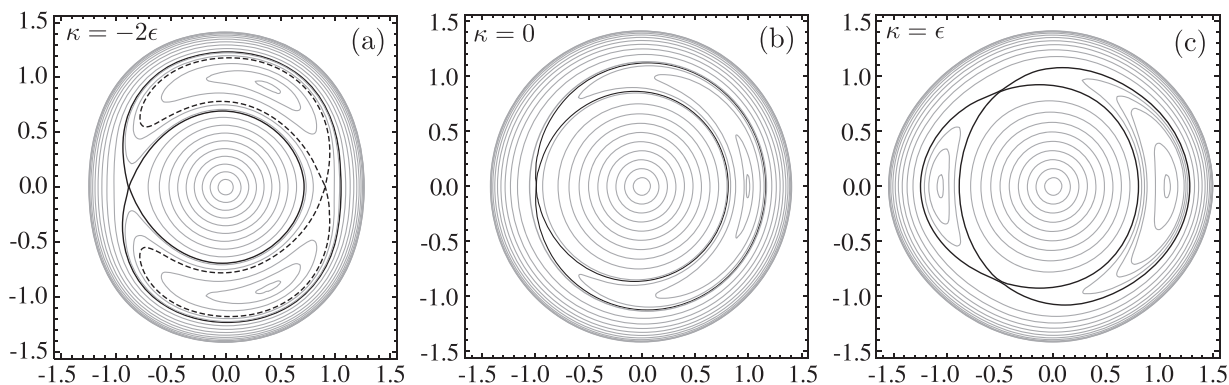


FIG. 5. Levels sets of  $\psi(r, x)$  from the approximated solution (11) with  $\epsilon = 0.1$  for different ellipticities  $\kappa$  (a)–(c).

toroidicity  $\epsilon$ , allowing a detailed study of the bifurcations that change the topology of the magnetic field. Now, we perform an asymptotic expansion of the nondimensional flux as  $\psi(r, \theta) = \psi_0(r, x) + \epsilon\psi_1(r, x) + O(\epsilon^2)$  and separate the problem in powers of the inverse aspect ratio  $\epsilon$ .

$$\Delta\psi_0 = (1 - 2r^2 + 2\kappa x^2), \tag{8}$$

$$\Delta\psi_1 = \partial_x\psi_0 + x(1 - 2r^2 + 2\kappa x^2), \tag{9}$$

with  $\Delta = \partial_x^2 + \partial_y^2$  the local Laplacian. Then we define  $\psi_0(r, x) = \bar{\psi}_0(r) + \kappa x^4/6$  and use  $\Delta\psi_0 = r^{-1}\partial_r(r\partial_r\psi_0(r))$ . The zero-order calculations give  $\bar{\psi}_0(r) = (1 - r^2/2)r^2/4$ . Consequently, the first order correction satisfies the equation

$$\Delta\psi_1 = \frac{x}{2} \left( 3 - 5r^2 + \frac{16}{3}\kappa x^2 \right). \tag{10}$$

Defining  $\psi_1(r, x) = \bar{\psi}_1(r, x) + 2\kappa x^5/15$  we have  $\Delta\bar{\psi}_1 = (3 - 5r^2)x/2$ . Now, we introduce the ansatz  $\bar{\psi}_1 = f(r)x$ , such that  $\Delta\bar{\psi}_1 = xr^{-3}\partial_r(r^3\partial_rf)$  and the first order problem is reduced to a simple ODE. After straightforward integrations and substitutions, we obtain the poloidal flux function to the first order in  $\epsilon$ .

$$\psi(r, x) = \left( 1 - \frac{1}{2}r^2 \right) \frac{r^2}{4} + \epsilon x \left( 1 - \frac{5}{9}r^2 \right) \frac{3r^2}{16} + \frac{\kappa}{6}x^4. \tag{11}$$

In Eq. (11) terms of the order  $O(\kappa\epsilon)$  are neglected, since we will consider only small ellipticities and  $\epsilon$  is already a small parameter. The structure of the magnetic surfaces depends on the number and the positions of the critical points ( $\nabla\psi = 0$ ), their type and the value of  $\psi$  on them. The origin  $r=0$ , is always an elliptic point between two critical points in the  $x$ -axis. The type of these points depends on the ellipticity  $\kappa$ . The condition for off-axis critical points  $|x_c| < r_c$  leads to  $|\kappa| \gtrsim \epsilon/8$ . In other words, the increase of the ellipticity in any direction causes the splitting of the on-axis critical points about  $|\kappa| \sim \epsilon/8$ , leading to a global change in the topology. In Figs. 5(a)–5(c), we plot the level sets of  $\psi$  obtained from the local solution (11) for different values of the ellipticity and in Fig. 6 we summarize the possible topologies in the parameter space. The system possesses one magnetic island for small ellipticities  $|\kappa| < \epsilon/8$ , two asymmetric islands for horizontally elongated plasmas ( $\kappa > \epsilon/8$ ) and one island

with internal separatrix for vertical elongations ( $\kappa < -\epsilon/8$ ). Also, in the limit of large vertical elongations ( $\kappa \ll 0$ ) the internal separatrix merges with the external one to form two symmetric islands.

Since the ellipticity and toroidicity define the island sizes and the equilibrium topology, they are related in a continuous way to the anisotropy  $\eta$ , defined before Eq. (4). As depicted in Fig. 7, increasing the vertical or horizontal elongation of the current density leads to a growth of the anisotropy of the current channels. However, the minimum  $\eta$  does not correspond to a vanishing ellipticity, but to a horizontally elongated state. This asymmetry between horizontal and vertical elongations is due to the toroidicity, which introduces an implicit anisotropy to the system in the non-elongated state. From this, the anisotropy only vanishes in the cylindrical case  $\epsilon \rightarrow 0$  (Fig. 7-right) and never becomes negative. Recall from Eq. (4) that positive anisotropies lead to  $I_+ > 2I_-$  as predicted for reversed monotonic current profiles before solving the analytical problem. The value of  $\eta$  is stationary during the bifurcation at  $\kappa = \epsilon/8$  where, briefly, a zero-current island is created.

If we consider a very small negative current density ( $\epsilon \rightarrow 0$ ), any finite ellipticity satisfy  $|\kappa| \gg \epsilon$  and the equilibrium presents two islands. This means that, if a quasi-stationary transition to an internal reversed current density is possible, the magnetic axis must simultaneously split into three separated axes. As the axes are aligned horizontally, this threefold splitting is not due to the up-down symmetry and may be expected in more general cases.

Now that we have introduced the main geometrical properties of the equilibrium we can discuss the force balance in configurations with multiple magnetic islands. The force balance condition requires  $\nabla p = \vec{j} \times \vec{B}$  everywhere inside the plasma. If we write the magnetic field and current density in its poloidal and toroidal components, the equilibrium equation may be casted like  $\nabla p = \vec{j}_p \times \vec{B}_\phi$

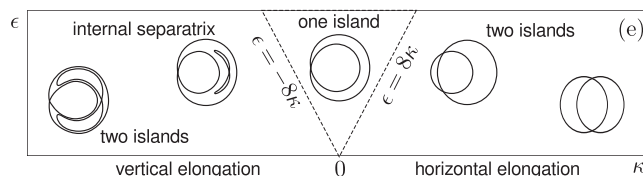


FIG. 6. Different topologies in the  $\kappa - \epsilon$  parameter space.

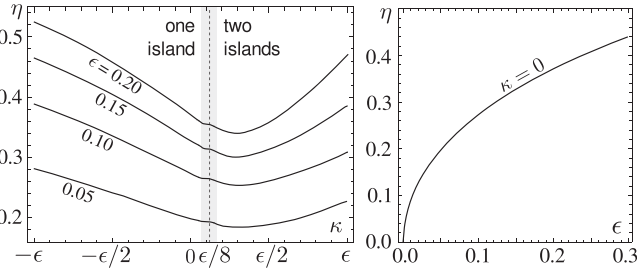


FIG. 7. Change in the anisotropy  $\eta$  as a function of the ellipticity  $\kappa$  for different values of  $\epsilon$  (left). Intrinsic anisotropy due to the toroidicity with zero ellipticity (right). The gray region is about the bifurcation value  $\kappa = \epsilon/8$  where  $\eta$  is stationary.

$+\vec{j}_\phi \times \vec{B}_p$ . From our local model, we can write explicitly the poloidal magnetic field as  $\vec{B}_p = \nabla\psi \times \nabla\phi$  to the first order in  $\epsilon$  and the toroidal current density  $j_\phi$  was previously introduced. On the other hand, the poloidal current and toroidal magnetic field depend on the arbitrary function  $F(\psi)$  through  $\vec{j}_p = \mu_0^{-1} \nabla F \times \nabla\phi$  and  $B_\phi = RF(\psi)$ , in consequence  $\vec{j}_p \times \vec{B}_\phi$  and  $\nabla p(\psi)$  depend on the particular equilibrium under consideration. Defining  $\vec{f} = \vec{j}_\phi \times \vec{B}_p = j_\phi \frac{\nabla\psi}{R}$ , we can write the force balance equation like

$$\nabla p + \frac{\mu_0^{-1}}{2R^2} \nabla F^2 = \vec{f}, \quad (12)$$

where only the right-hand side can be obtained from the local solution. Since  $\psi$  grow between the central magnetic axis and the secondary ones, the vector-field  $\vec{f}$  must invert its direction at the curve where the toroidal current density  $j_\phi$  vanishes, in consequence  $\vec{f}$  converges to every magnetic axis of the equilibrium. A particular configuration is depicted in the Fig. 8.

In a situation where the diamagnetic effects are small,  $F(\psi) \approx R_0 B_0$  is almost a constant and the second term of the left-hand side in Eq. (12) is small. In that limit  $\nabla p \approx \vec{f}$  and the pressure grows towards each magnetic axis. This corresponds to a good confinement since the pressure grows inwards the isobaric surfaces. In the general case the force balance includes the poloidal current and the pressure may vary in a different way, but for reasonable choices of the surface functions, the equilibrium may not differ much from this picture as there must be a concentration of particles in the channels to maintain their currents.

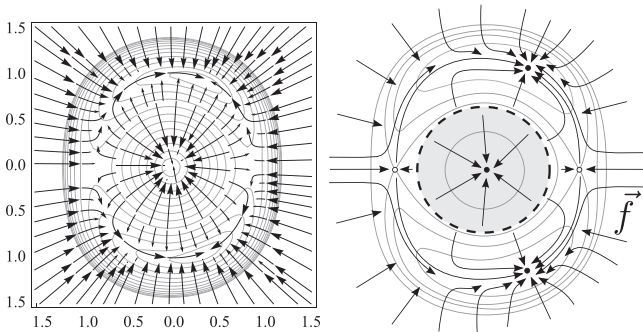


FIG. 8. Vector field  $\vec{f} = j_\phi \frac{\nabla\psi}{R}$  calculated from Eq. (11) for a configuration with two magnetic islands  $\{\kappa = -3\epsilon, \epsilon = 0.1\}$  (left). The main features of the vector field  $\vec{f}$  are depicted in the right, with the dashed line representing the curve where  $j_\phi = 0$  and  $\vec{f}$  inverts its direction.

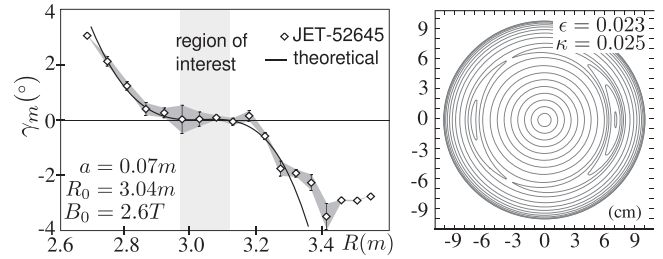


FIG. 9. Reproduction of experimental magnetic pitch angles in a current hole and reconstruction of the magnetic surfaces.

#### IV. DIAGNOSTIC ISSUES

One important issue in the description of CRECs is the identification of its experimental signatures as well as the non-conclusive diagnostics. For instance, in Fig. 9, we show that the flattening on the magnetic pitch angle profile  $\gamma_m$ , interpreted as a zero current density in Ref. 3 is also characteristic of a small current density inversion with two thin magnetic islands.

The theoretical curve in Fig. 9 was obtained from the local form of the poloidal flux (11). Considering the vacuum approximation we write the toroidal field as  $B_t = B_0 / (1 + \epsilon x)$ , so that the magnetic pitch angle, defined by  $\gamma_m = \arctan(B_p/B_t)$ , becomes

$$\gamma_m = \arctan(\tau |\nabla\psi|), \quad (13)$$

with  $\tau = \mu_0 a |j_0| / B_0$ . By a suitable choice of the region of interest and adjust of  $\kappa$  we can fit experimental measurements of the magnetic pitch angle obtained by Motional Stark Effect measurements about a current density minimum. The fitted experimental data are from Motional Stark Effect measurements reported in Hawkees *et al.* In this case, our model predicts  $j_0 \sim -42.6 \text{ kA/m}^2$  that is within the error of the zero value reported by Hawkees *et al.* The predicted size of the magnetic islands is below 2 cm, i.e., smaller than the spatial resolution of the measurement. In other words, additional diagnostics are required to discard the presence of a current density inversion when a broad flattening of  $\gamma_m$  is observed.

#### V. CONCLUSIONS

In summary, the non-nested magnetic topology resulting of current density reversals defines several current channels within the plasma. The ratio between the current in the positive channels and the central negative current depends on a topological parameter measuring the anisotropy of the positive channels. In general terms, the positive current is about twice the size of the central negative current causing the screening of this channel and forming a structure with net positive current. The anisotropy was shown to be related to the geometrical properties of the equilibrium in a region of interest inside the plasma. This was achieved by a local solution of the equilibrium problem without establishing any arbitrary function. It was observed that for a monotonic current density the anisotropy is always positive, indicating that the positive channels have *at least* twice the current magnitude of the negative one. In addition, the force balance analysis of

the local solutions shows good confinement properties for equilibria with multiple magnetic families. Finally, it was also shown that experimental magnetic pitch measures in a *current hole* are compatible with the existence of a small negative value of the current density and that additional diagnostics are required to discard the possibility of a current density reversal in configurations with deep current holes.

## ACKNOWLEDGMENTS

This work was partially supported by the National Council for Scientific and Technological Development (CNPq) - Brasil, grants 870198/1997-1 and 830577/1999-8 and the São Paulo Research Foundation (FAPESP) grants #2012/18073-1 and #2011/19296-1.

<sup>1</sup>B. J. D. Tubbing, N. A. C. Gottardi, B. J. Green, J. A. How, M. Huart, R. Konig, C. G. Lowry, P. J. Lomas, P. Noll, J. J. O'Rourke, P. H. Rebut, D. Stork, A. Tanga, A. Taroni, and D. J. Ward, *Nucl. Fusion* **32**, 967 (1992).

<sup>2</sup>J. Li, J. Luo, S. Wang, P. Fu, B. Shen, F. Liu, B. Wan, J. Shan, G. Xu, J. Huangand, J. Yu, J. Hu, Q. Yuan, and Y. Hu, *Nucl. Fusion* **47**, 1071 (2007).

<sup>3</sup>N. C. Hawkes, B. C. Stratton, T. Tala, C. D. Challis, G. Conway, R. DeAngelis, C. Giroud, J. Hobirk, E. Joffrin, P. Lomas, P. Lotte, J. Mailloux, D. Mazon, E. Rachlew, S. Reyes-Cortes, E. Solano, and K.-D. Zastrow, *Phys. Rev. Lett.* **87**, 115001 (2001).

<sup>4</sup>T. Fujita, T. Suzuki, T. Oikawa, A. Isayama, T. Hatae, O. Naito, Y. Sakamoto, N. Hayashi, K. Hamamatsu, S. Ide, and H. Takenaga, *Phys. Rev. Lett.* **95**, 075001 (2005).

<sup>5</sup>A. A. Martynov, S. Y. Medvedev, and L. Villard, *Phys. Rev. Lett.* **91**, 085004 (2003).

<sup>6</sup>S. Wang, *Phys. Rev. Lett.* **93**, 155007 (2004).

<sup>7</sup>P. Rodrigues and J. P. S. Bizarro, *Phys. Rev. Lett.* **95**, 015001 (2005).

<sup>8</sup>C. G. L. Martins, M. Roberto, I. L. Caldas, and F. L. Braga, *Phys. Plasmas* **18**, 082508 (2011).

<sup>9</sup>For any pair of coordinates  $\{u, v\}$  in a plane  $\phi = \text{const.}$ , the equation  $\partial_u \psi(u, v) = 0$  must lead to the same curve in the plane that  $\partial_v \psi(u, v) = 0$ . In addition, the curve must satisfy  $\psi(u, v) = \psi_0$ .

<sup>10</sup>J. P. Freidberg, *Rev. Mod. Phys.* **54**, 801 (1982).

<sup>11</sup>V. D. Shafranov, *Sov. Phys.-JETP* **26**, 682 (1960).

<sup>12</sup>H. Grad and H. Rubin, in *Proceedings of the Second United Nations International Conference on the Peaceful Uses of Atomic Energy* (Geneva, 1958), Vol. 31, p. 190.